Optically induced orbital polarization in bulk Ge and GaAs

F. Scali, M. Finazzi, F. Bottegoni, and C. Zucchetti [*]
Dipartimento di Fisica, Politecnico di Milano, Piazza Leonardo da Vinci 32, 20133 Milan, Italy

(Received 21 November 2025; accepted 7 April 2026; published 14 May 2026)

Optical orientation enables the injection of spin-polarized electron and hole populations in III-V and group-IV semiconductors. In particular, absorption of circularly polarized light near the direct gap generates spin-oriented electrons in the conduction band with polarization up to 50%, while hole polarization, opposite to that of electrons, can reach 83%. In recent years, increasing attention has focused on the orbital angular momentum, as charge-to-orbital conversion in semiconductors has been shown to be significantly more efficient than charge-to-spin. This has opened possibilities for exerting torques on ferromagnets in a semiconductive platform and is motivating research on the generation of carrier populations with net orbital angular momentum. In this framework, here, we exploit a "full-zone" $\mathbf{k} \cdot \mathbf{p}$ model to theoretically investigate the injection of orbital angular momentum in bulk Ge and GaAs by means of the absorption of circularly polarized photons. We show that the orbital polarization of holes considerably exceeds 100% for photon energies close to the direct gap of the semiconductors. These results offer a route for generating high orbital polarizations and suggest that semiconductors are a convenient platform for future development of orbitronic and opto-orbitronic devices.

DOI: 10.1103/c71s-44nt

I. INTRODUCTION

In the past decades, extensive efforts have focused on developing logic devices that exploit the spin degree of freedom to boost the performances of Si-based electronics [1] and add functionalities to the common digital devices. In this context, spin-transfer torque and spin-orbit torque magnetic random access memories represent a great success for spintronics, offering faster write/read speeds and lower power consumption compared with their charge-based counterpart [2]. These advances rely on the interplay between spin transport and the spin-charge interconversion properties of metals with large spin-orbit coupling, as Pt. At variance with storage devices, spin manipulation remains an elusive task: although electrical control of spin has been demonstrated in ferromagnet/normal-metal systems [3], the short spin lifetime of carriers still hinders the realization of all-electrical spin switch architectures.

Orbitronics, pioneered in 2005 [4], has recently emerged as a promising alternative [5–10]. Unlike spintronics, it exploits the orbital angular momentum of electrons or holes as the state variable. The generation, detection, and manipulation of orbital currents are therefore key objectives. To this aim, one can leverage the orbital-Hall effect (OHE) [9,11,12], the orbitronic counterpart of the spin-Hall effect (SHE) [13], in which a charge current generates transverse flow of orbital angular momentum. Significant OHE efficiencies have been reported in light metals Ti [6] and Cr [14], and in semiconductors like Ge [9] and Si [4,15]. These orbital currents can exert torques on ferromagnets, after orbit-to-spin conversion, bridging semiconductor technology and magnetism—previously limited by the low efficiency of SHE in semiconductors.

Within this framework, identifying efficient alternatives to generate orbital carriers is of great interest, and an attractive possibility is to exploit optical properties of semiconductors. Circularly polarized (CP) light, carrying spin angular momentum, is well known to induce net spin-polarized electron and hole populations in semiconductors [16,17], a process widely used for both fundamental and device-oriented studies [18]. Similarly, non-Gaussian beams designed in an optical vortex fashion carry a net orbital angular momentum [19] and have been proposed to generate spin and orbital currents through the photon-drag mechanism [19–22]. While this approach is conceptually appealing, the injected orbital polarization depends on the specific beam profile, and beam shaping/control can be experimentally demanding. A more accessible approach would be to exploit conventional CP light to directly generate orbitally polarized carriers, similarly to the optical spin orientation process.

In this article, we theoretically investigate the generation of orbital angular momentum in bulk Ge and GaAs through the absorption of CP photons, extending the optical orientation technique [16,17,23]. Using a "full zone" 30-band $\mathbf{k} \cdot \mathbf{p}$ model, we compute the bandstructure of the semiconductors over the entire first Brillouin zone (FBZ) and evaluate the carrier and orbital injection rates as function of incident photon energy. We find that near the direct gap, orbital accumulation in the conduction band remains below 1%, whereas it is as large as about 166% in the valence band, reflecting the p-type character of valence band states. These results demonstrate that bulk semiconductors naturally support strong orbital polarization and provide a robust platform for orbitronic architectures, capable of generating sizable orbital currents.

[*]Contact author: carlo.zucchetti@polimi.it

Published by the American Physical Society under the terms of the Creative Commons Attribution 4.0 International license. Further distribution of this work must maintain attribution to the author(s) and the published article's title, journal citation, and DOI.

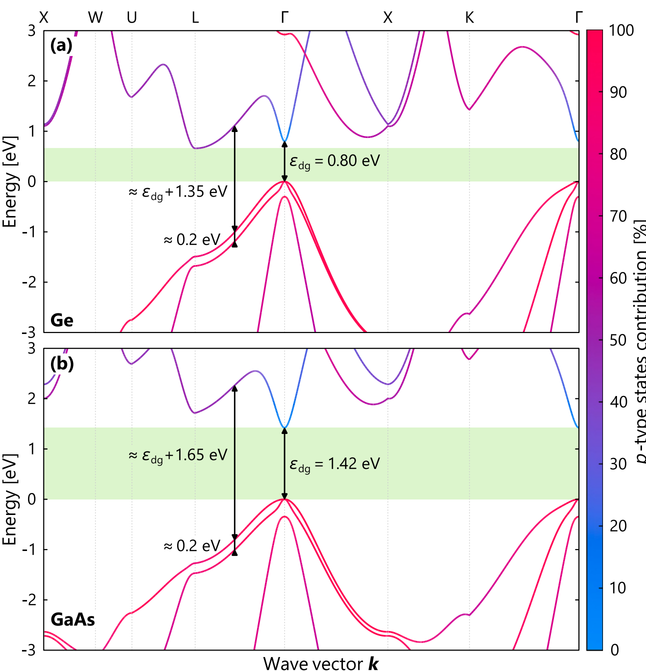

FIG. 1. Band structure of bulk Ge [panel (a)] and GaAs [panel (b)]. Green shaded area indicates the energy gap; the color at each **k** value indicates the contribution of p-type states to the band character.

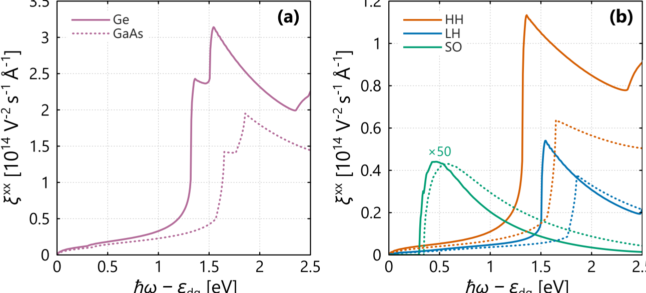

FIG. 2. (a) Total carrier injection tensor element ξ^{xx} as a function of the incident photon energy for Ge (solid line) and GaAs (dotted line). To ease the comparison, the value of ε_{dg} for each material has been subtracted from the photon energy. (b) Decomposition of the total carrier injection rate in contributions from the HH, LH, and SO bands for Ge (solid line) and GaAs (dotted line). Note that contribution from SO states has been multiplied by a factor of 50.

II. $k \cdot p$ MODEL

We have employed a $\mathbf{k} \cdot \mathbf{p}$ model including 30 states of s-, p-, and d- (e_g) type orbitals, which has proven effective in reproducing the band structure of bulk semiconductors across the full FBZ [24–29]. The eigenvalues, spin-orbit splitting parameters, and the matrix elements of the linear momentum have been taken from Ref. [26] for Ge and Ref. [25] for GaAs, and adapted to room-temperature conditions. The resulting band structures for Ge and GaAs are shown in Fig. 1, with the p-type character of the bands indicated by the color scale. As well known, in both semiconductors the valence band (VB) is almost fully made by p states, while the minimum of the conduction band (CB) at Γ is made by s-type orbitals. The minimum at L has a p-type character of ≈47% for both materials.

III. CARRIER INJECTION

Carrier injection rates can be calculated following the linear response model of Refs. [30,31]. The model considers the generation of carriers induced by a monochromatic electric field $\mathbf{E}(t) = \mathbf{E}(\omega)e^{-i\omega t} + \mathbf{E}^*(\omega)e^{i\omega t}$, where ω is the frequency, with $\hbar\omega \geqslant \varepsilon_{dg}$, ε_{dg} being the direct gap of Ge (0.80 eV) or GaAs (1.42 eV). Note that the vector $\mathbf{E}(\omega)$ is complex for elliptically polarized light. The generic component of the carrier injection tensor $\xi^{\alpha\beta}(\omega)$ is given by [30]

$$\xi^{\alpha\beta}(\omega) = \frac{2\pi e^2}{(\hbar\omega)^2} \sum_{c,v} \int \frac{d\mathbf{k}}{8\pi^3} v_{cv}^{\alpha*}(\mathbf{k})\, v_{cv}^{\beta}(\mathbf{k})\, \delta[\omega_{cv}(\mathbf{k}) - \omega], \tag{1}$$

where e is the electron charge, $\alpha, \beta \in \{x, y, z\}$ label the cartesian components along the cubic axes of the crystal, and $c(v)$ denotes the summation over the states of the CB (VB). The term v_{ij}^{α} represents the matrix element of the velocity operator $\hat{v}^{\alpha}$ along α between bands i and j at wave vector **k**: $\langle i, \mathbf{k}|\, \hat{v}^{\alpha}\, |j, \mathbf{k}'\rangle = v_{ij}^{\alpha}(\mathbf{k})\, \delta[\mathbf{k} - \mathbf{k}']$ [31]. Integration of Eq. (1) over the entire FBZ has been performed using the linear tetrahedron method [32], dividing the irreducible FBZ into ≈3.2×10^6 elements and accounting for the 48 symmetry operations of the O_h group. In cubic symmetry, the carrier injection tensor reduces to a single real-valued component $\xi^{xx} = \xi^{yy} = \xi^{zz}$. The calculated ξ^{xx} is shown in Fig. 2(a) for Ge (solid line) and GaAs (dotted line), with contributions from heavy hole (HH), light hole (LH), and split-off (SO) transitions displayed in Fig. 2(b). The peaks at $\hbar\omega - \varepsilon_{dg} \approx 1.35$ eV (1.65 eV) and $\hbar\omega - \varepsilon_{dg} \approx 1.55$ eV (1.85 eV) correspond to the ΓL absorption edges of Ge (GaAs), reflecting the large joint density of states for HH → CB and LH → CB transitions (see Fig. 1), respectively. The carrier injection rate follows $\dot{n} = \xi^{\alpha\beta}(\omega)E_{\alpha}^*(\omega)E_{\beta}(\omega)$, expressed using the Einstein summation convention over repeated indices [33]. It is worth mentioning that from ξ, the light absorption coefficient can be obtained as $\alpha(\omega) = \xi(\omega)\,\hbar\omega\,/\,(2n_{ri}\,c\,\epsilon_0)$ with n_{ri} refractive index, c speed of light, and ϵ_0 vacuum permittivity [34].

IV. ORBITAL ANGULAR MOMENTUM INJECTION

The components of the orbital injection pseudotensor $\eta_{e(h)}^{\alpha\beta\gamma}$ can be written as

$$\eta_{e}^{\alpha\beta\gamma}(\omega) = \frac{\hbar}{2}\frac{\pi e^2}{(\hbar\omega)^2} \sum_{c,\bar{c},v} \int \frac{d\mathbf{k}}{8\pi^3} L_{c\bar{c}}^{\alpha}(\mathbf{k})\, v_{cv}^{\beta*}(\mathbf{k})\, v_{\bar{c}v}^{\gamma}(\mathbf{k}) \times (\delta[\omega_{cv}(\mathbf{k}) - \omega] + \delta[\omega_{\bar{c}v}(\mathbf{k}) - \omega]) \tag{2}$$

and

$$\eta_{h}^{\alpha\beta\gamma}(\omega) = -\frac{\hbar}{2}\frac{\pi e^2}{(\hbar\omega)^2} \sum_{c,v,\bar{v}} \int \frac{d\mathbf{k}}{8\pi^3} L_{\bar{v}v}^{\alpha}(\mathbf{k})\, v_{cv}^{\beta*}(\mathbf{k})\, v_{c\bar{v}}^{\gamma}(\mathbf{k}) \times (\delta[\omega_{cv}(\mathbf{k}) - \omega] + \delta[\omega_{c\bar{v}}(\mathbf{k}) - \omega]) \tag{3}$$

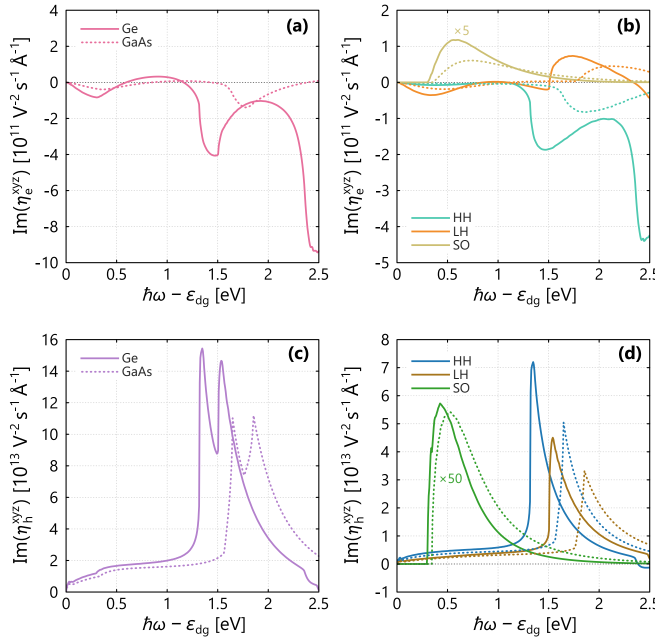

FIG. 3. (a) Electron orbital injection pseudotensor element $\eta_e^{xyz}(\omega)$ as a function of the incident photon energy. (b) Decomposition of $\eta_e^{xyz}(\omega)$ in contributions from the HH, LH, and SO bands. (c), (d) Same as panels (a) and (b) but for holes. Results for Ge and GaAs are indicated with continuous and dotted lines, respectively.

for electrons and holes, respectively. Here, $\bar{c}$ ($\bar{v}$) restricts the sum to degenerate or quasidegenerate couples of states for which $\hbar\omega_{c\bar{c}(v\bar{v})} < k_B T$, with the thermal energy set to $k_B T = 26$ meV in our calculations. This is done to account for the coherence between states as discussed in Ref. [31]. The term L_{ij}^{α} is the matrix element of the orbital angular momentum operator $\hat{L}^{\alpha}$ along α between bands i and j at wave vector $\mathbf{k}$: $\langle i, \mathbf{k} | \hat{L}^{\alpha} | j, \mathbf{k}' \rangle = \hat{L}_{ij}^{\alpha}(\mathbf{k})\, \delta[\mathbf{k} - \mathbf{k}']$. Owing to cubic symmetry, a unique independent and purely imaginary component exists: $\eta_{e(h)}^{xyz} = -\eta_{e(h)}^{xzy}$, along with cyclic permutations of the indices. The matrix elements of $\hat{L}^{\alpha}$ for the s, p, and d (e_g) orbitals used in the calculation satisfy $\langle s | \hat{L}^{\alpha} | s \rangle = \langle s | \hat{L}^{\alpha} | p, d \rangle = \langle p | \hat{L}^{\alpha} | d \rangle = 0$, while $\langle p | \hat{L}^{\alpha} | p \rangle$ are nonzero and given by

$$\hat{L}_{(p)}^{x} = \hbar \begin{pmatrix} 0 & 0 & 0 \\ 0 & 0 & -i \\ 0 & i & 0 \end{pmatrix}, \tag{4a}$$

$$\hat{L}_{(p)}^{y} = \hbar \begin{pmatrix} 0 & 0 & i \\ 0 & 0 & 0 \\ -i & 0 & 0 \end{pmatrix}, \tag{4b}$$

$$\hat{L}_{(p)}^{z} = \hbar \begin{pmatrix} 0 & -i & 0 \\ i & 0 & 0 \\ 0 & 0 & 0 \end{pmatrix}, \tag{4c}$$

with basis states $|p_x\rangle$, $|p_y\rangle$, and $|p_z\rangle$. Moreover, for $|d_{z^2}\rangle$ and $|d_{x^2-y^2}\rangle$ orbitals, $\langle d | \hat{L}^{\alpha} | d \rangle = 0$. The imaginary part of $\eta_{e(h)}^{xyz}(\omega)$ corresponding to the orbital components of the injection pseudotensor is shown for electrons and holes in Figs. 3(a) and 3(c), respectively, and panels (b) and (d) report the individual contributions from HH, LH, and SO

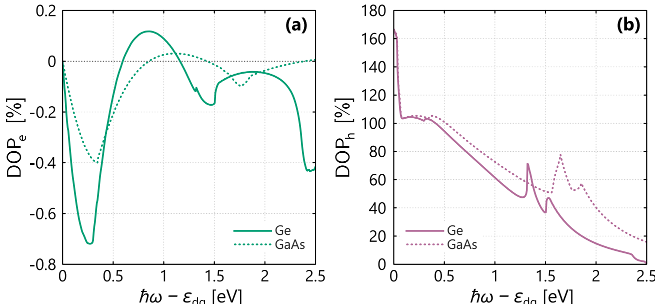

FIG. 4. Photon energy dependence of the degree of (a) electron orbital polarization $\mathrm{DOP_e}$ and (b) hole orbital polarization $\mathrm{DOP_h}$. Results for Ge and GaAs are indicated with continuous and dotted lines, respectively.

transitions. Note that the present model has been validated through calculations of the spin-injection pseudotensor, not shown here, which are consistent with previous reports [31], and show excellent agreement with experimental observations [29,35–37].

The orbital injection rate then reads

$$\dot{L}_{e(h)}^{\alpha}(\omega) = \mathrm{Re}\big[\eta_{e(h)}^{\alpha\beta\gamma}(\omega)\, E_{\beta}^{*}(\omega) E_{\gamma}(\omega)\big]. \tag{5}$$

A finite $\dot{L}$ arises only when two orthogonal field components are phase shifted, corresponding to elliptical polarization. For example, for right CP light $\mathbf{E}(\omega) = E_0(\mathbf{x} + i\mathbf{y})/\sqrt{2}$ the orbital injection rate result $\dot{L} = \eta^{zxy} E_x^* E_y + \eta^{zyx} E_y^* E_x$, corresponding to orbital polarization along z. Using $\eta^{zxy} = -\eta^{zyx} = \eta^{xyz}$, this reduces to $\dot{L}_{e(h)}^{z} = \mathrm{Im}[\eta_{e(h)}^{xyz}]\, {E_0}^2$. Similarly, it can be shown that left CP produces an opposite orbital injection, while linear polarization yields zero. Thus, for the same optical power, the orbital injection rate scales linearly with the degree of circular polarization of the light. Further, in the following, we do not distinguish the direction of $\dot{L}_{e(h)}$, since, due to the cubic symmetry, the orbital polarization aligns with the propagation of the circularly polarized light with the same magnitude.

V. DISCUSSION

The degree of orbital polarization (DOP) for electrons and holes quantifies the fraction of injected carriers with net orbital polarization. It is defined as $\mathrm{DOP}_{e(h)} = \dot{L}_{e(h)}/\dot{n}$. For purely CP light, from previous considerations, this expression simplifies to $\mathrm{DOP}_{e(h)} = \mathrm{Im}[\eta_{e(h)}^{xyz}(\omega)]/\xi^{xx}(\omega)$. The resulting value of DOP is plotted in Fig. 4 as a function of the incident photon energy. It is worth mentioning that $\mathrm{DOP_h}$ in Fig. 4 exceeds 100% because it is expressed in $\hbar/2$ units in Eqs. (2) and (3). This convention enables direct comparison between the magnitudes of orbital angular momentum with the spin one, without changing units.

A simple atomic picture helps interpret the obtained results. At the Γ point, the electronic states of Ge and GaAs can be expressed in terms of atomic s and p orbitals. Table I lists their total angular momentum quantum numbers together with the corresponding spherical harmonics expansions. Momentum conservation implies that the absorption of CP photons results in a change of angular momentum

TABLE I. Total angular momentum quantum numbers and spherical harmonics expansion of the wavefunctions at the Γ point.

Band	$\|j, m_j\rangle$	Spherical harmonics expansion
CB	$\|1/2, 1/2\rangle$	$Y_0^0 \|\uparrow\rangle$
	$\|1/2, -1/2\rangle$	$Y_0^0 \|\downarrow\rangle$
LH	$\|3/2, 1/2\rangle$	$\sqrt{1/3}\, Y_1^1 \|\downarrow\rangle + \sqrt{2/3}\, Y_1^0 \|\uparrow\rangle$
	$\|3/2, -1/2\rangle$	$\sqrt{1/3}\, Y_1^{-1} \|\uparrow\rangle + \sqrt{2/3}\, Y_1^0 \|\downarrow\rangle$
HH	$\|3/2, 3/2\rangle$	$-Y_1^1 \|\uparrow\rangle$
	$\|3/2, -3/2\rangle$	$Y_1^{-1} \|\downarrow\rangle$
SO	$\|1/2, 1/2\rangle$	$\sqrt{2/3}\, Y_1^1 \|\downarrow\rangle - \sqrt{1/3}\, Y_1^0 \|\uparrow\rangle$
	$\|1/2, -1/2\rangle$	$\sqrt{2/3}\, Y_1^{-1} \|\uparrow\rangle - \sqrt{1/3}\, Y_1^0 \|\downarrow\rangle$

$\Delta m_j = (+)-1$ for left (right) circular polarization. For electrons, however, excitation at $\hbar\omega = \varepsilon_{dg}$ invariably populates s-like ($l = 0$) conduction-band states at Γ, yielding $DOP_e = 0$. Even at photon energies above ε_{dg}, DOP_e remains small because p-like contributions to conduction states are minor. In contrast, for holes with, e.g., left-handed CP light at $\hbar\omega = \varepsilon_{dg}$, HH ($m_l = 1$) and LH ($m_l = 0, 1$) states are involved in optical transitions (see Table I) with relative intensity 3:1 as known from the optical orientation technique [17]. Specifically, for HH states $\langle 3/2, 3/2| L^z |3/2, 3/2\rangle = \hbar$ and for LH states $\langle 3/2, 1/2| L^z |3/2, 1/2\rangle = 1/3\,\hbar$. Thus, for photon energies resonant with the direct gap, $DOP_h = (3\hbar + 1/3\,\hbar)/4$, leading to $DOP_h = 10/6 = 166\%$ in unit of $\hbar/2$. For higher photon energies, the increasing weight of $m_l = 0$ states reduces the DOP_h value, which nonetheless remains above 40% for photon energies lower than 2.2 eV (3.4 eV) for Ge (GaAs) [see Fig. 4(b)].

VI. CONCLUSION

In conclusion, we have theoretically demonstrated that circularly polarized light induces not only spin but also orbital accumulation in bulk Ge and GaAs. While the spin polarization in the conduction band is known to be significant, the orbital polarization is $<1\%$ due to the s-like character of the conduction states. Conversely, the valence band exhibits a remarkably large orbital polarization. These results suggest that the Ge and GaAs valence band could be effectively exploited to generate orbital angular momentum in semiconductors for applications in orbitronic architectures.

DATA AVAILABILITY

The data that support the findings of this article are openly available [38].

[1] I. Žutić, J. Fabian, and S. D. Sarma, Spintronics: Fundamentals and applications, Rev. Mod. Phys. **76**, 323 (2004).

[2] G. Prenat, K. Jabeur, P. Vanhauwaert, G. D. Pendina, F. Oboril, R. Bishnoi, M. Ebrahimi, N. Lamard, O. Boulle, K. Garello, J. Langer, B. Ocker, M.-C. Cyrille, P. Gambardella, M. Tahoori, and G. Gaudin, Ultra-fast and high-reliability SOT-MRAM: From cache replacement to normally-off computing, IEEE Trans. Multi-Scale Comput. Syst. **2**, 49 (2016).

[3] K. Ando, S. Takahashi, K. Harii, K. Sasage, J. Ieda, S. Maekawa, and E. Saitoh, Electric manipulation of spin relaxation using the spin Hall effect, Phys. Rev. Lett. **101**, 036601 (2008).

[4] B. A. Bernevig, T. L. Hughes, and S.-C. Zhang, Orbitronics: The intrinsic orbital current in p-doped silicon, Phys. Rev. Lett. **95**, 066601 (2005).

[5] G. Sala and P. Gambardella, Giant orbital Hall effect and orbital-to-spin conversion in $3d$, $5d$, and $4f$ metallic heterostructures, Phys. Rev. Res. **4**, 033037 (2022).

[6] Y. G. Choi, D. Jo, K. H. Ko, D. Go, K. H. Kim, H. G. Park, C. Kim, B. C. Min, G. M. Choi, and H. W. Lee, Observation of orbital Hall effect in a light metal Ti, Nature (London) **619**, 52 (2023).

[7] D. Jo, D. Go, G.-M. Choi, and H.-W. Lee, Spintronics meets orbitronics: Emergence of orbital angular momentum in solids, npj Spintron. **2**, 19 (2024).

[8] T. Adamantopoulos, M. Merte, D. Go, F. Freimuth, S. Blügel, and Y. Mokrousov, Orbital Rashba effect as a platform for robust orbital photocurrents, Phys. Rev. Lett. **132**, 076901 (2024).

[9] E. Santos, J. E. Abrão, J. L. Costa, J. G. S. Santos, G. Rodrigues-Junior, J. B. S. Mendes, and A. Azevedo, Negative orbital Hall effect in germanium, Phys. Rev. Appl. **22**, 064071 (2024).

[10] E. S. Santos, J. E. Abrão, J. L. Costa, J. G. S. Santos, K. R. Mello, A. S. Vieira, T. C. R. Rocha, T. J. A. Mori, R. O. R. Cunha, J. B. S. Mendes, and A. Azevedo, Bulk and interface effects based on Rashba-like states in Ti and Ru nanoscale-thick films: Implications for orbital-charge conversion in spintronic devices, ACS Appl. Nano Mater. **8**, 4300 (2025).

[11] J. H. Cullen, H. Liu, and D. Culcer, Giant orbital Hall effect due to the bulk states of 3D topological insulators, npj Spintron. **3**, 22 (2025).

[12] A. Veneri, T. G. Rappoport, and A. Ferreira, Extrinsic orbital Hall effect: Orbital skew scattering and crossover between diffusive and intrinsic orbital transport, Phys. Rev. Lett. **134**, 136201 (2025).

[13] J. E. Hirsch, Spin Hall effect, Phys. Rev. Lett. **83**, 1834 (1999).

[14] I. Lyalin, S. Alikhah, M. Berritta, P. M. Oppeneer, and R. K. Kawakami, Magneto-optical detection of the orbital Hall effect in chromium, Phys. Rev. Lett. **131**, 156702 (2023).

[15] R. Matsumoto, R. Ohshima, M. Funato, Y. Ando, D. Go, Y. Mokrousov, and M. Shiraishi, Observation of orbital Hall effect in Si, arXiv:2501.14237.

[16] G. Lampel, Nuclear dynamic polarization by optical electronic saturation and optical pumping in semiconductors, Phys. Rev. Lett. **20**, 491 (1968).

[17] R. Allenspach, F. Meier, and D. Pescia, Optical orientation of electrons in surface states, Phys. Rev. Lett. **51**, 2148 (1983).

[18] P. A. Dainone, N. F. Prestes, P. Renucci, A. Bouché, M. Morassi, X. Devaux, M. Lindemann, J.-M. George, H. Jaffrès, A. Lemaitre, *et al.*, Controlling the helicity of light by electrical magnetization switching, Nature (London) **627**, 783 (2024).

[19] G. F. Q. Rosen, P. I. Tamborenea, and T. Kuhn, Interplay between optical vortices and condensed matter, Rev. Mod. Phys. **94**, 035003 (2022).

[20] G. F. Quinteiro and P. I. Tamborenea, Twisted-light-induced optical transitions in semiconductors: Free-carrier quantum kinetics, Phys. Rev. B **82**, 125207 (2010).

[21] A. A. Gunyaga, M. V. Durnev, and S. A. Tarasenko, Photocurrents induced by structured light, Phys. Rev. B **108**, 115402 (2023).

[22] O. J. G. Sanchez, G.-H. Peng, W.-H. Li, C.-H. Shih, C.-H. Chien, and S.-J. Cheng, Enhanced photo-excitation and angular-momentum imprint of gray excitons in WSe_2 monolayers by spin-orbit-coupled vector vortex beams, ACS Nano **18**, 11425 (2024).

[23] F. Bottegoni, C. Zucchetti, G. Isella, M. Bollani, M. Finazzi, and F. Ciccacci, Spin-orbit interaction and spin-charge conversion in semiconductors, Riv. Nuovo Cim. **43**, 45 (2020).

[24] M. Cardona and F. H. Pollak, Energy-band structure of germanium and silicon: The $k \cdot p$ method, Phys. Rev. **142**, 530 (1966).

[25] S. Richard, F. Aniel, and G. Fishman, Energy-band structure of Ge, Si, and GaAs: A thirty-band $\mathbf{k} \cdot \mathbf{p}$ method, Phys. Rev. B **70**, 235204 (2004).

[26] D. Rideau, M. Feraille, L. Ciampolini, M. Minondo, C. Tavernier, H. Jaouen, and A. Ghetti, Strain-induced changes in the band structure of silicon: A first-principles study, Phys. Rev. B **74**, 195208 (2006).

[27] N. Fraj, I. Saïdi, S. Ben Radhia, and K. Boujdaria, Band structures of AlAs, GaP, and SiGe alloys: A 30 $k \times p$ model, J. Appl. Phys. **102**, 053703 (2007).

[28] Z. Song, W. Fan, C. S. Tan, Q. Wang, D. Nam, D. H. Zhang, and G. Sun, Band structure of $Ge_{1-x}Sn_x$ alloy: A full-zone 30-band $k \cdot p$ model, New J. Phys. **21**, 073037 (2019).

[29] P. Mudi, S. K. Khamari, S. Khan, C. Zucchetti, F. Bottegoni, and T. K. Sharma, Full-zone optical spin injection in $Al_xGa_{1-x}As$ alloys, J. Phys. D: Appl. Phys. **58**, 015108 (2025).

[30] F. Nastos, J. Rioux, M. Strimas-Mackey, B. S. Mendoza, and J. E. Sipe, Bulk photogalvanic effects in semiconductors, Phys. Rev. B **76**, 205113 (2007).

[31] J. Rioux and J. E. Sipe, Optical injection and control of spin and orbital angular momentum in semiconductors, Phys. Rev. B **81**, 155215 (2010).

[32] H. Jeschke, *Computational Methods in Solid State Theory: SS 2016* (Frankfurt am Main, Germany, 2016).

[33] A. Najmaie, R. D. R. Bhat, and J. E. Sipe, All-optical injection and control of spin and electrical currents in quantum wells, Phys. Rev. B **68**, 165348 (2003).

[34] J. L. Cheng, J. Rioux, J. Fabian, and J. E. Sipe, Theory of optical spin orientation in silicon, Phys. Rev. B **83**, 165211 (2011).

[35] C. Rinaldi, M. Cantoni, M. Marangoni, C. Manzoni, G. Cerullo, and R. Bertacco, Wide-range optical spin orientation in Ge from near-infrared to visible light, Phys. Rev. B **90**, 161304(R) (2014).

[36] F. Pezzoli, A. Balocchi, E. Vitiello, T. Amand, and X. Marie, Optical orientation of electron spins and valence-band spectroscopy in germanium, Phys. Rev. B **91**, 201201(R) (2015).

[37] F. Bottegoni, C. Zucchetti, G. Isella, E. Pinotti, M. Finazzi, and F. Ciccacci, Modeling the photo-induced inverse spin-Hall effect in Pt/semiconductor junctions, J. Appl. Phys. **124**, 033902 (2018).

[38] F. Scali, M. Finazzi, F. Bottegoni, and C. Zucchetti, Data regarding the manuscript: Optically induced orbital polarization in bulk Ge and GaAs [Data set], Zenodo (2026), doi:10.5281/zenodo.19481064.